NUMERICAL SIMULATION ON TWO-TEMPERATURE CHEMICALLY NON-EQUILIBRIUM STATES IN DECAYING SF_6 ARCS AFTER APPLICATION OF RECOVERY VOLTAGE

Y TANAKA[1], K SUZUKI[2]

[1]Faculty of Electrical and & Computer Eng., Kanazawa Univ., JAPAN.
[2]Department of Electrical Engineering, Tokyo Denki Univ., JAPAN.
tanaka@ec.t.kanazawa-u.ac.jp

ABSTRACT

This paper describes calculation results by the developed two-temperature (2T) chemically non- equilibrium (CNE) model for a decaying SF_6 arc plasma with transient recovery voltage (TRV) application. The developed model solves energy equations for electrons and heavy particles, mass conservation equations for each of 19 species in SF_6 arc plasmas, accounting for totally 122 reactions. Transient distributions of electron temperature and heavy particle temperature as well as CNE composition were obtained for a decaying SF_6 arc plasma considering non-equilibrium effects.

1. INTRODUCTION

The high-voltage gas circuit breaker extinguishes an SF_6 arc plasma formed between the electrodes during a high current interruption by blowing SF_6 gas to the arc. To downsize such a circuit breaker and to enhance its reliability, it is necessary to understand in detail arc interruption phenomena in SF_6 gas. One powerful tool for this purpose is numerical modeling of decaying SF_6 arcs. We have so far developed a self-consistent chemically non-equilibrium (CNE) model for decaying arc plasmas [1]−[4]. That work found that consideration of CNE effects were important to determine the particle composition especially around the fringe of the arc plasma [4]. Furthermore, we have developed a two-temperature (2T) CNE model for decaying SF_6 arc plasmas [5]. From those results, it was confirmed that application of transient recovery voltage (TRV) to the arc raise the electron temperature T_e more rapidly than heavy particle temperature T_h, i.e. gas temperature [5].

In this paper, the developed model for decaying SF_6 arcs is briefly described with consideration of not only CNE but also thermally non-equilibrium, i.e. 2T effects. The calculation results are shown on spatial distribution and temporal variations in the T_e and the T_h. Finally, the particle composition were also demonstrated including electron density n_e and F^- density n_{F^-} in decay phase in SF_6 arc plasmas under TRV application condition.

2. Modeling of SF_6 arc plasmas in two-temperature chemically non-equilibrium state

2.1. Assumptions

The developed model assumes the following conditions in the SF_6 arc plasma for simplicity: (i) The plasma has axisymmetric structure. (ii) The gas flow is laminar. (iii) Optically thin condition was assumed. (iv) Electron emission phenomena were not considered. (v) Evaporation of the electrode and the nozzle was neglected. (vi) 19 species like SF_6, SF_5, SF_4, SF_3, SF_2, SF, S_2, F_2, S, F, SF^+, S_2^+, F_2^+, SF^-, S^+, F^+, S^-, F^-, and e^- were taken into account as constituents in SF_6 arc plasmas. (vii) The T_e can be different from the T_h. (viii) Electrons, ions, and neutral particles have the same flow velocity. (ix) Quasi-neutrality for electronic charge were assumed.

2.2. Governing equations

According to these assumptions the behavior of SF_6 arc plasmas is considered to be governed by the following equations:

Mass:

$$\frac{D\rho}{Dt} = -\rho(\nabla \cdot \boldsymbol{u}), \tag{1}$$

Momentum:

$$\rho\frac{D\boldsymbol{u}}{Dt} = -\nabla p + \nabla \cdot \boldsymbol{\tau}, \tag{2}$$

$$\boldsymbol{\tau} = \tau_{ij} = 2\eta\left[e_{ij} - \frac{1}{3}\delta_{ij}(\nabla \cdot \boldsymbol{u})\right] \tag{3}$$

Energy for heavy particles:

$$\rho_h C_{vh}\frac{DT_h}{Dt} = -p_h(\nabla \cdot \boldsymbol{u}) + \nabla \cdot \left(\lambda_{tr}^h \nabla T_h\right) + Q_{e-h} + Q_{heat}^h \tag{4}$$

$$Q_{heat}^h = \sum_{j=1(j\neq e)}^{N} \nabla\cdot(\rho D_j h_j \nabla Y_j) + \sum_{\ell=1(\beta_{c\ell}^l \cdot \beta_{c\ell}^r = 0)}^{L} \Delta Q_\ell \tag{5}$$

Energy for electrons:

$$\frac{3}{2}kn_{\mathrm{e}}\frac{DT_{\mathrm{e}}}{Dt} = \nabla\cdot(\lambda^{\mathrm{e}}_{\mathrm{tr}}\nabla T_{\mathrm{e}}) - Q_{\mathrm{e-h}} + Q^{\mathrm{e}}_{\mathrm{heat}} \quad (6)$$

$$Q^{\mathrm{e}}_{\mathrm{heat}} = \nabla\cdot(\frac{1}{m_{\mathrm{e}}}\frac{5}{2}kT_{\mathrm{e}}\boldsymbol{\Gamma}_{\mathrm{e}}) + \sum_{\ell=1(\beta^{\mathrm{f}}_{e\ell}\cdot\beta^{\mathrm{r}}_{e\ell}\neq 0)}^{L}\Delta Q_{\ell} + \sigma_{\mathrm{e}}|E|^2 - P_{\mathrm{rad}} - Q^{\mathrm{e}}_{\mathrm{exc}} \quad (7)$$

Mass of species j:

$$\rho\frac{DY_j}{Dt} = \nabla\cdot(\rho D_j\nabla Y_j) + S_j, \quad (8)$$

$$S_j = m_j\sum_{\ell}^{L}(\beta^{\mathrm{r}}_{j\ell}-\beta^{\mathrm{f}}_{j\ell})\left(k^{\mathrm{f}}_{\ell}\prod_{i=1}^{N}n_i^{\beta^{\mathrm{f}}_{i\ell}} - k^{\mathrm{r}}_{\ell}\prod_{i=1}^{N}n_i^{\beta^{\mathrm{r}}_{i\ell}}\right) \quad (9)$$

The equation of state:

$$p = p_{\mathrm{e}} + p_{\mathrm{h}} \quad (10)$$

$$p_{\mathrm{e}} = n_{\mathrm{e}}kT_{\mathrm{e}} \quad (11)$$

$$p_{\mathrm{h}} = \sum_{j(j\neq\mathrm{e})}^{N} n_j kT_{\mathrm{h}} \quad (12)$$

Mass density:

$$\rho = \frac{p}{k\frac{Y_{\mathrm{e}}}{m_{\mathrm{e}}} + k\sum_{j=1(j\neq\mathrm{e})}^{N}\frac{Y_j}{m_j}T_{\mathrm{h}}} \quad (13)$$

Energy conversion by excitation:

$$Q^{\mathrm{e}}_{\mathrm{exc}} = \sum_{j=1(j\neq\mathrm{e})}^{N}\left[k(T^j_{\mathrm{ex}})^2\frac{\partial\ln Z_j(T^j_{\mathrm{ex}})}{\partial T^j_{\mathrm{ex}}} - kT_{\mathrm{h}}^2\frac{\partial\ln Z_j(T_{\mathrm{h}})}{\partial T_{\mathrm{h}}}\right]\nu_{\mathrm{eh}}n_{\mathrm{e}} \quad (14)$$

Energy conversion by elastic collision:

$$Q_{\mathrm{e-h}} = \sum_{j=1(j\neq\mathrm{e})}^{N}\frac{3}{2}k(T_{\mathrm{e}}-T_{\mathrm{h}})\frac{2m_jm_{\mathrm{e}}}{(m_j+m_{\mathrm{e}})^2}\nu_{\mathrm{eh}}n_{\mathrm{e}} \quad (15)$$

Effective reaction heat:

$$\Delta Q_{\ell} = E_{\mathrm{reac}\ell}\left(k^{\mathrm{f}}_{\ell}\prod_{i=1}^{N}n_i^{\beta^{\mathrm{f}}_{i\ell}} - k^{\mathrm{r}}_{\ell}\prod_{i=1}^{N}n_i^{\beta^{\mathrm{r}}_{i\ell}}\right) \quad (16)$$

where ρ: mass density, t: time, $\boldsymbol{u}$: gas flow vector, p: pressure, $\boldsymbol{\tau}$: stress tensor, η: viscosity, e_{ij}: unit tensor, δ_{ij}: Kronecker delta, T: temperature, C_{vh}: effective specific heat at constant volume for heavy particles, λ_{tr}: translational thermal conductivity, D_j: effective diffusion coefficient, h_j: enthalpy of species j, Y_j: mass fraction of species j, P_{rad}: radiation power, ΔQ_{ℓ}: heating power from reaction heat of reaction ℓ, m_j: mass of species j, $\beta_{j\ell}$: stoichiometric coefficient of species j for reaction ℓ, $k^{\mathrm{f,r}}_{\ell}$: reaction rate coefficient for reaction ℓ, n_j: density of species j, ν_{eh}: collision frequency between the electron and heavy particles, $E_{\mathrm{reac}\ell}$: Reaction heat for reaction ℓ, k: Boltzmann constant, $\frac{D}{Dt} = \frac{\partial}{\partial t} + \boldsymbol{u}\cdot\nabla$ is the Lagrangian derivative. As seen in Eq. (6), the energy conversion by excitation reactions was also considered equivalently using the effective excitation temperature T^j_{ex} for species j [6].

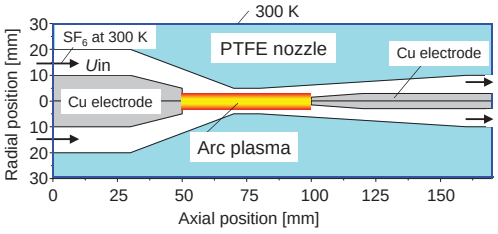

Fig. 1. Calculation domain.

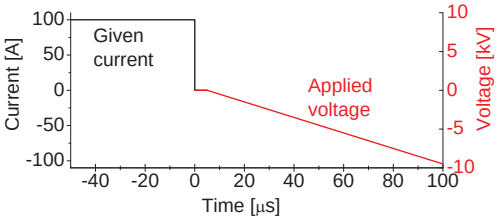

Fig. 2. Given current and applied voltage.

2.3. Properties and conditions

The thermodynamic and transport properties were self-consistently calculated using the computed non-equilibrium composition, both T_{e} and T_{h}, and the collision integrals at each position at each calculation step. The developed model took into account 122 reactions including their backward reactions [1],[7]. Figure 1 illustrates the calculation space in this paper. The nozzle and the electrode has a non-slip wall with condition $\boldsymbol{u}=\boldsymbol{o}$. At the inlet around axial position z=0 mm, the gas flow and the temperature were set 10 m/s and 300 K, respectively. The pressure at one point of the outlet was fixed at 0.5 MPa. Figure 2 shows the current and applied voltage given in the calculation. First, the steady state calculation was made for a current of dc 100 A. Then, the transient state calculation was made for a current stepped down from 100 A to 0 A at t=0 μs. From t=5μs, the transient recovery voltage (TRV) was applied with a rise of rate of recovery voltage (RRRV). The reason why a 5 μs delay was set before TRV application is that TRV application without a delay caused the large current flowing in the arc. The value of RRRV for this paper is 0.1 kV/μs. Transient calculation was conducted using the C-CUP algorithm.

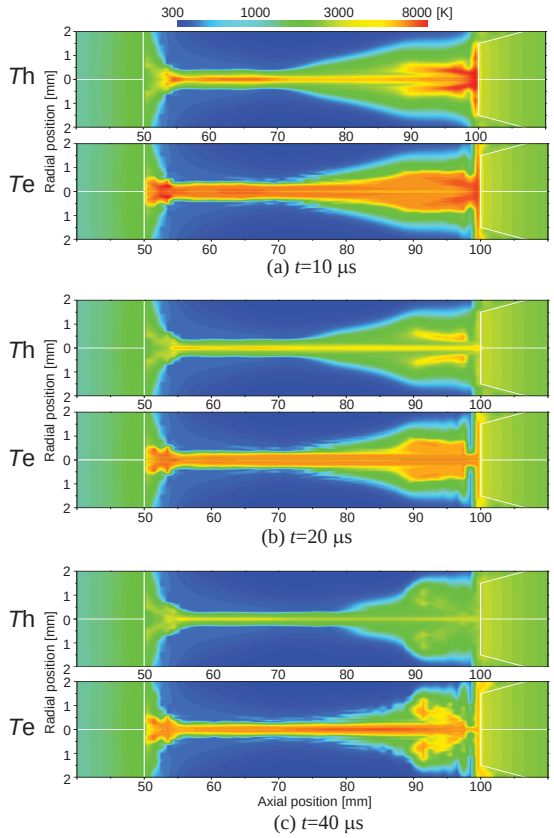

Fig. 3. Transient spatial distribution in the electron temperature and the heavy particle temperature between the electrodes in an SF_6 arc at RRRV=0.1 kV/μs.

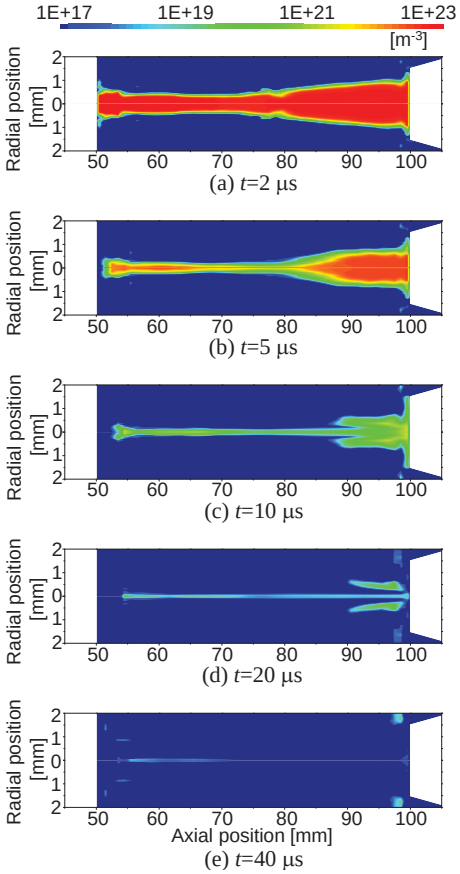

Fig. 4. Electron density distribution in an SF_6 arc at RRRV=0.1 kV/μs.

3. Results

Figure 3 depicts the T_h and T_e in an SF_6 arc at t = 10, 20 and 40 μs. The TRV has a RRRV=0.1 kV/μs after t=5 μs. This condition of RRRV=0.1 kV/μs corresponds to successful interruption condition under which the arc plasma continues to decay, while RRRV=0.2 kV/μs involves interruption failure. At t=10 μs, the applied voltage reaches to 0.5 kV between the electrodes for RRRV=0.1 kV/μs. As seen in this figure, there is a region of $T_e > T_h$. This is because TRV application accelerates the electrons in the arc plasma, resulting in higher T_e than T_h rather than relaxation process from electrons to heavy particles. At t >10 μs, T_e continues to increase while T_h is decreased by the energy loss for heavy particles. At t=40 μs, T_e is obviously 2000 K higher than T_h around the axis, i.e. the 2T state occurs.

It is essential to understand the n_e which affects determines several kinds of electron impact reactions, and finally the electrical conductivity of the plasmas. In addition, it is said that n_e is affected by the electron attachment to F in an SF_6 arc. Thus, attention is paid to n_e and n_{F^-}. Figures 4 and 5 present the spatial distribution of the n_e and n_{F^-} between the electrodes. At t=2 μs, the arc plasma has high n_e about 10^{23} m^{-3} on the axis, while n_{F^-} reaches 10^{21} m^{-3} around the arc fringe. After that, n_e decreases with time drastically especially around the axial position z ~70–80 mm. Electrons around the arc fringe are trapped with F to increase n_{F^-}. This is due mainly to the dissociative electron attachment reaction $F_2 + e \rightarrow F^- + F$. On the other hand, TRV is applied after t=5 μs. However, n_e continues to decrease with time in this condition. The n_{F^-} is hardly changed with time.

Particle composition variation in radial direction at nozzle throat z=70 mm is plotted in Fig. 6 for t=5, 10 and 20 μs. At t=5 μs, SF_6 is seen to be dissociated to produce several products such as SF_4, SF_3 and SF_2 etc at radial positions r < 0.7

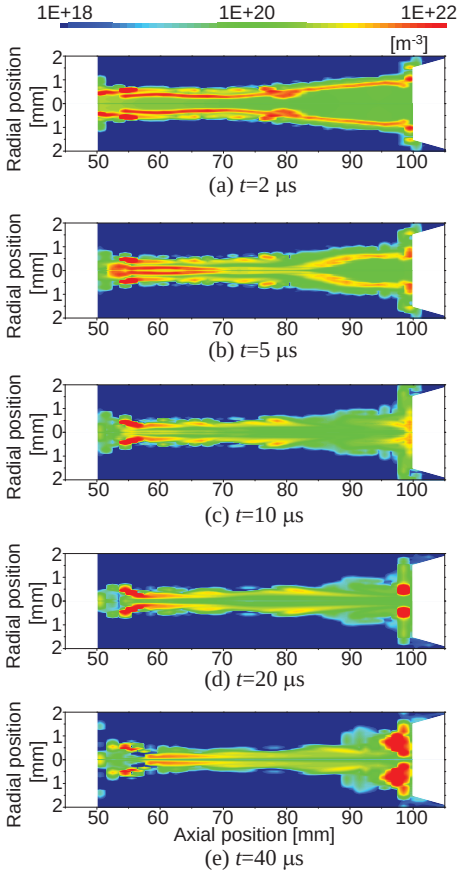

Fig. 5. F- density distribution in an SF_6 arc at RRRV=0.1 kV/μs.

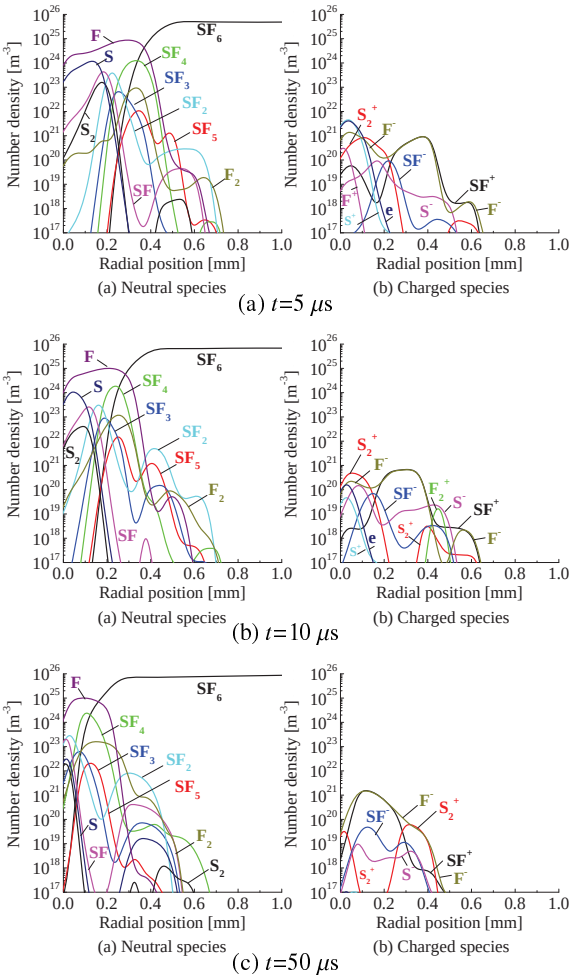

Fig. 6. Radial distribution of composition in an SF_6 arc at RRRV=0.1 kV/μs.

mm. On the axis, F atom is dominant for neutral species, while the electron is predominant for charged particles. At t >10 μs, n_e decreases with time markedly, being lower than densities of S_2^+ and F^-. At t=50 μs, n_e is much lower than 10^{17} m^{-3} while n_{F^-} keeps ~10^{20} m^{-3}. This means that electrons were trapped with F through the electron attachment with F_2 and SF.

4. Summary

A two-dimensional numerical thermo-fluid model of SF_6 arc plasmas was developed with consideration of not only CNE effects but also 2T effects self-consistently. Two energy equations for electrons and heavy particles were separately solved to obtain the behaviors of electron temperature T_e and heavy particle temperature T_h. Results showed that 2T state and CNE effects were clearly seen in a residual SF_6 arc plasma in case of TRV application with RRRV=0.1 kV/μs.

The authors would like to express our thanks to Dr. T. Shinkai and Mr. T. Iijima for their disscussions on SF_6 circuit breakers.

References

[1] Y.Tanaka, K.Suzuki, *Proc. the First Int. Conf. Electric Power Equip. Switching Technol., ICEPE2011*, pp.492–495, 2011.

[2] Y.Tanaka, T.Shinkai, *Int.Conf. Electr. Eng., ICEE2012*, P-PS1-1 , 2012.

[3] Y.Tanaka, T.Shinkai, *Proc. 19th Int.Conf. Gas Discharges & their Appl., GD2012*, pp.66–69, 2012.

[4] Y.Tanaka, K.Suzuki, IEEE Trans. Power Delivery, Vol.28, Issue 4, pp.2623-2629, 2013.

[5] Y. Tanaka, et al., Int. Conf. Electric Power Equip. ICEPE2013, 2-p1-P-2, 2013.10, Matsue, Japan

[6] Y. Tanaka, et al., *IEEE Trans. Plasma Sci.*, **25**, 991–995, 1997.

[7] I.Coll, et al., *J. Phys. D: Appl. Phys.*, **33**, 221–229, 2000.